Chromosomal Protein HMGN1 Modulates Histone H3 Phosphorylation

ARTICLE *in* MOLECULAR CELL · SEPTEMBER 2004

Impact Factor: 14.02 · DOI: 10.1016/j.molcel.2004.08.006 · Source: PubMed

Molecular Cell, Vol. 15, 573–584, August 27, 2004, Copyright ©2004 by Cell Press

Chromosomal Protein HMGN1 Modulates Histone H3 Phosphorylation

Jae-Hwan Lim, Frédéric Catez, Yehudit Birger, Katherine L. West, Marta Prymakowska-Bosak, Yuri V. Postnikov,* and Michael Bustin
Laboratory of Metabolism
National Cancer Institute
National Institutes of Health
Bethesda, Maryland 20892

Summary

Here we demonstrate that HMGN1, a nuclear protein that binds to nucleosomes and reduces the compaction of the chromatin fiber, modulates histone posttranslational modifications. In *Hmgn1*$^{-/-}$ cells, loss of HMGN1 elevates the steady-state levels of phospho-S10-H3 and enhances the rate of stress-induced phosphorylation of S10-H3. In vitro, HMGN1 reduces the rate of phospho-S10-H3 by hindering the ability of kinases to modify nucleosomal, but not free, H3. During anisomycin treatment, the phosphorylation of HMGN1 precedes that of H3 and leads to a transient weakening of the binding of HMGN1 to chromatin. We propose that the reduced binding of HMGN1 to nucleosomes, or the absence of the protein, improves access of anisomysin-induced kinases to H3. Thus, the levels of posttranslational modifications in chromatin are modulated by nucleosome binding proteins that alter the ability of enzymatic complexes to access and modify their nucleosomal targets.

Introduction

Posttranslational modifications of histones play a key role in regulating nuclear processes occurring in the context of chromatin and serve as a specific code that facilitates diverse cellular processes including the orderly progression of the cell cycle, the cellular response to external signals, and the induction of specific gene expression (Jenuwein and Allis, 2001; Strahl and Allis, 2000; Turner, 2002). The phosphorylation of serine 10 in histone H3 (S10-H3) is one of the best-characterized links between histone modification and functional changes in chromatin. This modification may disrupt interactions between the positively charged H3 tail and the DNA backbone or serve as a recognition site for recruitment of regulatory factors. S10-H3 phosphorylation is associated with genes engaged in active transcription (Barratt et al., 1994; Chadee et al., 1999; Labrador and Corces, 2003; Sassone-Corsi et al., 1999) and may facilitate further histone modifications that are associated with transcriptional events in chromatin (Davie and Spencer, 2001). Phosphorylation of S10-H3 is also closely linked to chromatin condensation during mitosis and meiosis (Cheung et al., 2000) and serves as a hallmark for mitotic chromosomes. In addition, phosphorylation of S10-H3 is associated with the transduction of external signals to chromatin leading to the transient expression of immediate-early (IE) genes (Mahadevan et al., 1991; Thomson et al., 1999a).

The phosphorylation of H3 is mediated by several specific kinases, activated by distinct pathways. For example, mammalian mitotic H3 phosphorylation is associated with Aurora B kinases (Clayton and Mahadevan, 2003), H3 phosphorylation by IKK-α is important for the activation of NF-κB (Yamamoto et al., 2003), and the IE gene response is mediated mainly by MSK1 and MSK2 (Soloaga et al., 2003), although RSK-2 has also been implicated in this process (Davie, 2003; Sassone-Corsi et al., 1999). The activity of these kinases could be affected by nucleosome binding proteins such as histone H1 or HMGN, which alter the compactness of the chromatin fiber and affect the interaction of chromatin modifiers with their nucleosomal targets. Indeed, H1 inhibits the activity of ATP-dependent chromatin-remodeling enzymes (Horn et al., 2002), the mitotic phosphorylation of H3 (Shibata and Ajiro, 1993), and the PCAF-mediated acetylation of H3 (Herrera et al., 2000). The inhibition of the remodeling enzymes was linked to changes in the higher-order chromatin structure, while the inhibition of the acetylation was linked to steric hindrance by the positively charged C-terminal of H1. Likewise, the binding of HMGN proteins to nucleosome cores affects the PCAF-mediated acetylation of histone H3 (Herrera et al., 1999). Thus, architectural nucleosome binding proteins may modulate the interaction of chromatin-modifying enzymes with their chromatin targets.

Treatment of fibroblasts with growth factors such as EGF, or protein synthesis inhibitors such as anisomycin, results in a rapid and transient phosphorylation of histone H3 and of the nonhistone HMGN1, an effect named "nucleosomal response" (Clayton and Mahadevan, 2003; Mahadevan et al., 1991; Thomson et al., 1999a). In the nucleosomal response, the stimuli that lead to phosphorylation of S10 and S28 in H3 also phosphorylate serine 6 in HMGN1 (Barratt et al., 1994; Soloaga et al., 2003), a major member of the HMGN nucleosome binding protein family (Bustin, 2001). The close temporal link between the nucleosomal response and the induction of immediate-early gene expression suggested that these phosphorylation events are important steps in the cascade leading to gene induction. The phosphorylation of HMGN1 may potentially be very significant because during the nucleosomal response all of the cellular S6 in HMGN1, but only a small fraction of the H3, is phosphorylated (Clayton et al., 2000). Although the events leading to HMGN1 phosphorylation have been described in detail, the role of this modification in signaling to chromatin targets is not understood.

HMGN is a family of proteins that binds specifically to the 147 base pair nucleosome core particle, the building block of the chromatin fiber (Bustin, 2001). The binding of these proteins to nucleosomes reduces the compaction of the chromatin fiber and alters the transcription, replication, and repair potential of chromatin templates (Birger et al., 2003; Bustin, 2001). HMGN proteins have a modular structure and contact both the nucleosomal DNA and the histone through multiple interaction sites (Bustin, 2001). A central, positively charged region con-

*Correspondence: yupo@helix.nih.gov

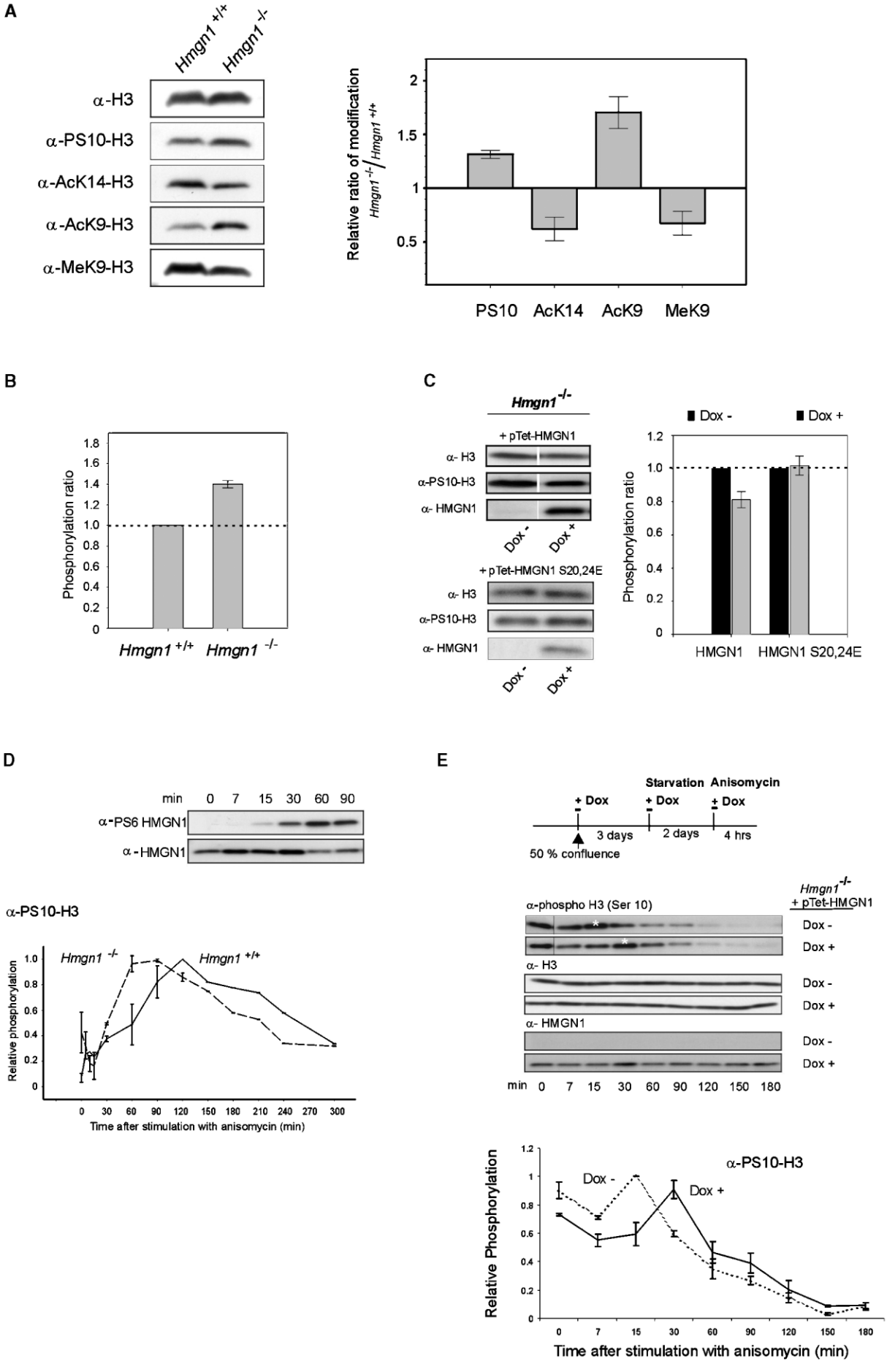
A
Hmgn1 +/+
Hmgn1 -/-
α-H3
α-PS10-H3
α-AcK14-H3
α-AcK9-H3
α-MeK9-H3
Relative ratio of modification
Hmgn1 -/- / Hmgn1 +/+
PS10
AcK14
AcK9
MeK9
B
Phosphorylation ratio
Hmgn1 +/+
Hmgn1 -/-
C
Hmgn1 -/-
+ pTet-HMGN1
α- H3
α-PS10-H3
α- HMGN1
Dox -
Dox +
+ pTet-HMGN1 S20,24E
Phosphorylation ratio
HMGN1
HMGN1 S20,24E
D
min 0 7 15 30 60 90
α-PS6 HMGN1
α- HMGN1
α-PS10-H3
Hmgn1 -/-
Hmgn1 +/+
Relative phosphorylation
Time after stimulation with anisomycin (min)
E
Starvation
Anisomycin
+ Dox
3 days
2 days
4 hrs
50 % confluence
α-phospho H3 (Ser 10)
Hmgn1 -/-
+ pTet-HMGN1
α- H3
α- HMGN1
min 0 7 15 30 60 90 120 150 180
α-PS10-H3
Relative Phosphorylation
Time after stimulation with anisomycin (min)

tains the major HMGN-chromatin contacts (Crippa et al., 1992; Trieschmann et al., 1995); however, additional sites of interactions have been identified. Thus, site-directed crosslinking of HMGN-nucleosome complexes indicates that the C-terminal region of HMGN1 is located near the amino terminal tail of histone H3, while the N-terminal region contacts H2B (Trieschmann et al., 1998). The close association between HMGN1 and H3 could affect the ability of enzymes to modify residues in the histone tails.

Here we use *Hmgn1*$^{-/-}$ mouse embryonic fibroblasts (MEFs) and in vitro reconstitution experiments to test the possibility that HMGN1 modulates the phosphorylation of H3 and to examine directly the role of HMGN1 phosphorylation during the nucleosomal response in regulating the IE gene response. We find that loss of HMGN1 alters the steady-state phosphorylation levels of H3 and demonstrate that the binding of HMGN1 to nucleosomes inhibits the phosphorylation of H3. We demonstrate that during the nucleosomal response the phosphorylation of HMGN1 precedes that of H3 and weakens the binding of HMGN1 to nucleosomes in living cells. The absence of HMGN1 enhances the rate of H3 phosphorylation and alters the expression of several IE genes. We conclude that the binding of HMGN1 to nucleosomes inhibits the rate of H3 phosphorylation and suggest that the interaction of HMGN proteins and similar architectural chromatin binding proteins with nucleosomes modulates the pattern of posttranslational modifications in the tails of core histones.

Results

Altered Levels of Phospho S10-H3 in *Hmgn1*$^{-/-}$ Cells

To test whether the presence of HMGN1 protein is related to the levels of posttranslational modifications in the amino terminal tail of histone H3, we used commercial antibodies specific to modified residues to examine histones isolated from *Hmgn1*$^{+/+}$ or *Hmgn1*$^{-/-}$ mouse embryonic fibroblasts (MEF) (Birger et al., 2003). Western analysis with proteins extracted from the two cell types, grown to the same density under identical conditions, revealed that loss of HMGN1 protein altered the level of posttranslational modification at several amino acid residues in the amino terminus of H3 (Figure 1A). We focused our attention on the phosphorylation levels at serine 10 in the tail of histone H3 (S10-H3), a well-studied modification associated with mitotic entry, gene expression, and the transduction of external signals to nucleosomes. In multiple tests with both primary and immortalized fibroblasts, the steady-state levels of phosphorylated S10-H3 were significantly (20%–40%) higher in *Hmgn1*$^{-/-}$ cells as compared to *Hmgn1*$^{+/+}$ cells (Figure 1B), an indication that the presence of HMGN1 protein affects this histone modification.

To verify that the increased rate of H3 phosphorylation is indeed due to loss of HMGN1 protein, we established revertant *Hmgn1*$^{-/-}$ MEFs expressing either the wild-type HMGN1 protein or the double point mutant HMGN1-S20,24E, both under the control of the inducible tetracycline response element (TRE) promoter, i.e., *Hmgn1*$^{-/-}$ *Tre*$^{+/+}$ MEFs. Adding doxycycline (Dox) to these cells gradually increased the amount of protein to levels comparable to those of HMGN1 in wild-type cells (Westerns in Figure 1C). The steady-state levels of phosphorylated S10-H3 in the *Hmgn1*$^{-/-}$*Tre*$^{+/+}$ cells expressing wild-type HMGN1 grown in the presence of Dox and expressing HMGN1 were about 20% lower than in cells grown in the absence of Dox (bar graph in Figure 1C), an indication that the phosphorylation levels of H3 are indeed linked to the presence of HMGN1 protein. In contrast, induction of the HMGN1-S20,24E mutant which enters the nucleus but does not bind to chromatin (Prymakowska-Bosak et al., 2001) did not change the steady-state P-S10-H3 levels (Figure 1C). Thus, the reexpression of HMGN1 and the interaction of the protein with chromatin lower the levels of P-S10-H3, i.e., reverts the *Hmgn1*$^{-/-}$ phenotype to normal.

Loss of HMGN1 Enhances the Rate of S10-H3 Phosphorylation upon Induction of Immediate-Early Gene Expression

To study the possible role of HMGN1 protein in regulating the levels of P-S10-H3, we analyzed the kinetics of

Figure 1. Loss of HMGN1 Enhances the Phosphorylation of S10-H3

(A) Loss of HMGN1 alters the levels of posttranslational modifications in the tail of H3. Shown are Westerns with the antibodies indicated on the left of each panel set. In each set, the signal was normalized to the amount of total histone H3 extracted from the same cell type (i.e., *Hmgn1*$^{-/-}$ or *Hmgn1*$^{+/+}$). The ratios of the relative levels of modifications in primary *Hmgn1*$^{-/-}$ to *Hmgn1*$^{+/+}$ MEFs, obtained from three independent experiments, are shown in the bar graph.

(B) Enhanced P-S10-H3 levels in *Hmgn1*$^{-/-}$ MEFs. Signal intensities normalized to total H3.

(C) Restoration of WT phenotype by reexpression of wild-type but not mutant HMGN1 protein. Western analysis of extracts from *Hmgn1*$^{-/-}$ cells stably transfected with inducible plasmids expressing HMGN1 or HMGN1-S20,24E protein under the control of the Tet promoter. Induction of HMGN1, but not of HMGN1-S20,24E, expression by doxycycline (Dox) reduces the levels of phospho-H3.

(D) Loss of HMGN1 enhances the rate of S10-H3 phosphorylation during the nucleosomal response. Extracts of *Hmgn1*$^{+/+}$ or *Hmgn1*$^{-/-}$ cells, various times after stimulation with anisomycin, were analyzed by Westerns with either anti-H3 or anti-P-S10-H3 antibody. The values of phosphorylated H3 intensities were normalized with the intensities of total H3 and scaled from 0 to 1. The graph summarizes the results of at least three experiments performed with different clones. The inset is Western analysis demonstrating phosphorylation of Serine 6 of HMGN1 (with anti-PS6 HMGN1) during the nucleosomal response.

(E) Analysis of phosphorylated histone H3 levels after anisomycin induction in *Hmgn1*$^{-/-}$ revertant cells expressing Dox-inducible HMGN1 protein. The scheme of the experiment is shown on the top. *Hmgn1*$^{-/-}$ MEFs grown to 50% confluence were either treated or not treated with Dox (Dox^{+} or Dox^{-}) to either induce or not induce HMGN1 expression. After starving the cells for 2 days, the cells were treated with anisomycin and the levels of P-S10-H3 analyzed by Westerns. Shown are Western analyses with the antibodies indicated on top of each panel. The white asterisk in the anti-P-S10-H3 panels points out the maximum signal intensity. The values of phosphorylated H3 intensities were normalized with the intensities of total H3 and scaled from 0 to 1. Note that the experiments in panel (D) and (E) were done with primary and transformed cells, respectively.

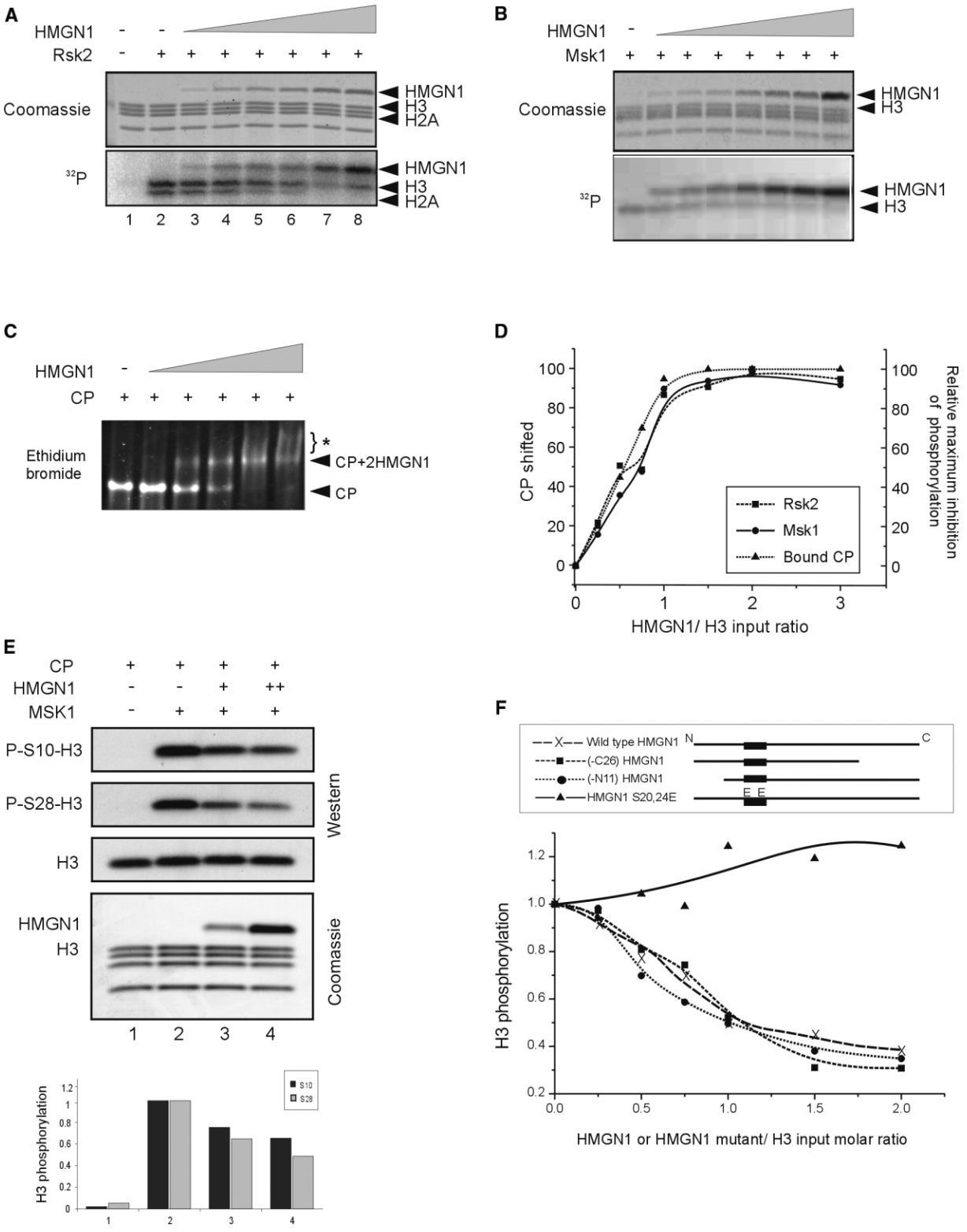

Figure 2. HMGN1 Inhibits the Phosphorylation of Nucleosomal H3

(A) Inhibition of RSK2. Coomassie blue stained 15% polyacrylamide SDS-containing gels, and corresponding autoradiograms (^{32}P) of reaction mixtures containing equal amounts of CP reconstituted with increasing amounts of HMGN1, followed by incubation with [γ-^{32}P]ATP and RSK2. Note the inverse correlation between HMGN1 input and H3 phosphorylation.

(B) Inhibition of MSK1.

(C) Specific binding of HMGN1 to CP. EtBr-stained native 4.5% polyacrylamide gels of the reaction mixture analyzed in lanes 2–7 of (A). The migration of the CP and the CP associated with 2 molecules of HMGN1 is indicated on the right. Asterisk, the region containing nonspecific complexes of CP with more than 2 molecules of HMGN1.

phosphorylation of S10-H3 in *Hmgn1*$^{+/+}$ or *Hmgn1*$^{-/-}$ MEFs after anisomycin-induced stimulation of IE gene expression. This process involves the transient phosphorylation of S10 in H3 and S6 in HMGN1 (Barratt et al., 1994). In *Hmgn1*$^{-/-}$ MEFs, both the onset and the peak of phosphorylation of S10-H3 occurred earlier than in *Hmgn1*$^{+/+}$ MEFs (Figure 1D). Immediately after stimulation, the P-S10-H3 level in *Hmgn1*$^{-/-}$ MEFs decreased, but within 15 min the level of phosphorylation rapidly increased and peaked 60 min after induction. In *Hmgn1*$^{+/+}$ MEFs, the initial drop in the P-S10-H3 level was small and subsequently increased at a lower rate, peaking only 90–120 min after induction (graph in Figure 1D). These results suggest that loss of HMGN1 enhances the rate at which S10-H3 is phosphorylated, a finding that is in agreement with our observations of the steady-state P-S10-H3 levels in growing cells (Figures 1A–1C).

The "nucleosomal response" in our MEFs was similar to that observed in other systems (Soloaga et al., 2003; Thomson et al., 1999b) and led to the phosphorylation of both S10-H3 and S6 in HMGN1. In *Hmgn1*$^{+/+}$ cells, the levels of P-S6 in HMGN1 peaked 60 min after exposure to 50 ng/ml anisomycin (Western in Figure 1D). Under the same conditions, the phosphorylation of S10 in H3 peaked 120 min after induction (graph in Figure 1D), suggesting that in wild-type MEFs the phosphorylation of HMGN1 precedes that of H3 (see also Figure 5).

To further test the involvement of HMGN1 in the phosphorylation of S10-H3, we grew *Hmgn1*$^{-/-}$*Tre*$^{+/+}$ cells in either the absence or presence of Dox (experimental scheme in Figure 1E). After 3 days, the cells grown in the presence of Dox contained HMGN1 levels comparable to those present in wild-type cells. We then starved the cells for 48 hr, also in the presence or absence of Dox, and induced the nucleosomal response by anisomycin treatment. These transformed cells maintained a relative-high level of phosphorylated H3 even after 48 hr of starvation. Nevertheless, we repeatedly observed (note the low standard deviations) that immediately after anisomycin treatment the levels of P-S10-H3 transiently dropped and the specific activity was reduced by 20%. The cells lacking HMGN1 recovered faster and reached their maximum P-S10-H3 levels 15 min after stimulation, while the revertant cells expressing HMGN1 reached their peak 30 min after stimulation (Figure 1E). Thus, reexpression of HMGN1 reduced the rate of anisomycin-induced phosphorylation of S10-H3. Taken together, the results suggest that the presence of HMGN1 impedes the phosphorylation of S10 in H3.

HMGN1 Inhibits the Phosphorylation of Nucleosomal but Not Free H3

To understand the mechanism whereby HMGN1 interferes with the phosphorylation of H3, we incubated purified nucleosome core particles (CP) with increasing amounts of HMGN1 and a constant amount of ^{32}P-ATP, and tested whether HMGN1 affects the activity of RSK2 and MSK1, two kinases implicated in the mitogen- and stress-induced phosphorylation of S10-H3. The levels of phosphorylation were determined by quantitative analysis of protein gels and their corresponding autoradiograms. HMGN1 inhibited both the RSK2 (Figure 2A)- and the MSK1 (Figure 2B)-mediated H3 phosphorylation in a dose-dependent manner. Mobility shift assays of the reaction mixtures indicated that HMGN1 bound to the CP and generated complexes containing 2 HMGN1 per CP (CP+2HMGN1 in Figure 2C). Significantly, the HMGN-mediated inhibition of both MSK1 and RSK2 correlated with the binding of HMGN1 to CPs. The inhibition was dose dependent up to the point at which the nucleosome binding sites were saturated by HMGN1 and the maximum inhibition of phosphorylation coincided with the HMGN1 concentration that bound all the CPs specifically (Figure 2D). Higher concentrations of HMGN1, which bind to CPs nonspecifically and form large molecular weight complexes that smear on native gels (asterisk in Figure 2C), did not cause additional inhibition of enzymatic activity. HMGN1 inhibited the phosphorylation of both S10 and S28 (Figure 2E), the two major MSK1 targets in the amino-terminal tail of H3. We also note that both MSK1 and RSK2 phosphorylated efficiently HMGN1 and that HMGN1 also inhibited the phosphorylation of histone H2A (Figure 2A).

The inhibition of H3 phosphorylation required binding of HMGN1 to nucleosomes since the HMGN1-S20,24E double mutant, which does not bind to nucleosomes (Prymakowska-Bosak et al., 2001), did not inhibit the MSK1-mediated H3 phosphorylation (Figure 2F). In contrast, the HMGN1-ΔC26 and the ΔN11-HMGN1 deletion mutants which lack the C-terminal or the N-terminal region of the protein, respectively, but bind to nucleosomes (Trieschmann et al., 1995), inhibited the MSK1-mediated phosphorylation with the same efficiency as the wild-type protein (Figure 2F). Thus, the nucleosomal binding domain, which is the major site of interaction between HMGN1 and the nucleosome (Crippa et al., 1992), is also the major protein region that interferes with the ability of MSK1 to phosphorylate H3.

HMGN proteins bind specifically to chromatin but not to DNA or histones. Therefore, to further verify that histone H3 phosphorylation is inhibited by HMGN1 only in nucleosomal context and the inhibition is indeed specific, we repeated these experiments using free, rather than nucleosomal, histone H3 as substrates. Both RSK2 and MSK1 phosphorylated free H3 much more efficiently than nucleosomal H3. Nucleosomal H3 was phosphorylated significantly less while free H3 was phosphorylated significantly more than HMGN1 (compare Figure 2A and 2B to Figure 3A and 3B).

(D) The inhibition of H3 phosphorylation requires binding of HMGN1 to nucleosomes. The relative phosphorylation and the CP-HMGN1 interactions were quantified by scanning the autoradiograms in (A) and (B), and the EtBr gel in (C) and plotted against the HMGN1/H3 input ratio. The left y axis depicts the relative amount of CP shifted, while the right y axis depicts the relative phosphorylation levels. Note that the maximum inhibition corresponds to the maximum CP shifted.

(E) HMGN1 inhibits the MSK1, mediated phosphorylation of both S10-H3 and S28-H3. Shown are Western analyses with the antibodies specific to the epitopes indicated on the left. Western with anti-H3 and the protein gel indicate equal loading of CP particles.

(F) The inhibition of H3 phosphorylation requires binding of HMGN1 to nucleosomes. Shown is a graph of the effect of HMGN1 and HMGN1 mutants (see box above the graph) on the specific activity of the phosphorylated H3.

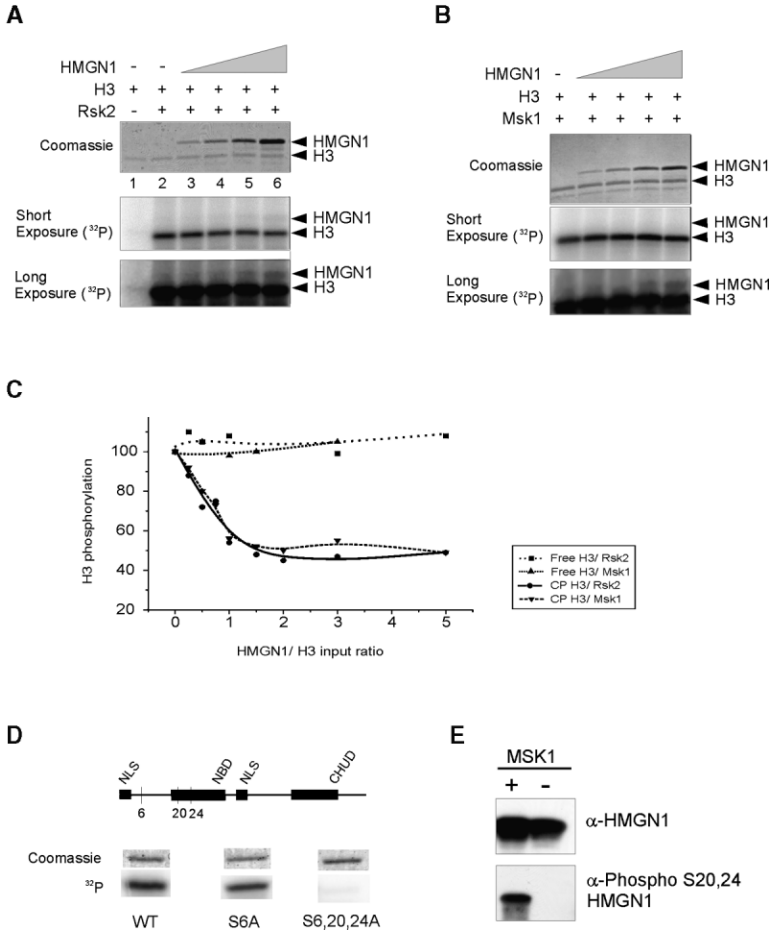

Figure 3. HMGN1 Does Not Inhibit the Phosphorylation of Free H3

Coomassie blue-stained 15% polyacrylamide SDS-containing gels and corresponding autoradiograms (^{32}P) of reaction mixtures containing increasing amounts of HMGN1 and a constant amount of H3 phosphorylated with [γ-^{32}P]ATP by either RSK2 (A) or MSK1 (B). Visualization of HMGN1 phosphorylation requires long exposures since free H3 is phosphorylated very efficiently.

(C) Graph of the effect of HMGN1 on the relative H3 phosphorylation levels after incubation of free or nucleosomal H3 with RSK2 or MSK1. Data for CP phosphorylation are from Figure 2. Nonnucleosomal bound H3 is phosphorylated to a higher degree than HMGN1.

(D) MSK1 phosphorylates serines located in the nucleosomal binding domain of HMGN1. Shown are Coomassie blue-stained 15% polyacrylamide SDS-containing gels and corresponding autoradiograms (^{32}P) of reaction mixtures containing equal amounts of either wild-type HMGN1 or the S6A or S6,20,24A point mutants phosphorylated with [γ-^{32}P] ATP and MSK1. An outline of the protein domain structure is shown above the gel. NLS, nuclear localization signal; NBD, nucleosome binding domain; CHUD, chromatin unfolding domain.

(E) Westerns with the antibodies indicated on the right side of HMGN1 either treated or untreated with MSK1.

The phosphorylation of free H3 by either RSK2 or MSK1 was not affected by HMGN1 even when the concentration of HMGN1 was several fold higher than that of H3 (Figures 3A and 3B). The plots of specific activity of H3 phosphorylation as a function of the HMGN1/H3 input ratio clearly indicated that HMGN1 inhibits the RSK2- and MSK1- mediated phosphorylation of nucleosomal but not of free histone H3 (Figure 3C). Thus, the inhibition is most likely due to steric factors associated with the binding of HMGN1 to CP rather than to a direct interaction or inactivation of the kinases by HMGN1. Indeed, it is known that the binding of HMGN to nucleosomes involves several contacts, including the amino termini of the core histones (Crippa et al., 1992), and that part of HMGN1 is in close proximity to the amino terminus of H3 (Trieschmann et al., 1998).

Rapid Decrease in HMGN1 Chromatin Binding upon IE Gene Induction

RSK2 and MSKs are the major kinases implicated in the nucleosomal response (Sassone-Corsi et al., 1999; Soloaga et al., 2003). These enzymes are known to phosphorylate serine 6 in HMGN1, and we demonstrated that RSK2 does not phosphorylate S20 and S24 located in the nucleosomal binding domain of HMGN1 (Prymakowska-Bosak et al., 2001). During our studies with an HMGN1 S6A point mutant, we noted that MSK1 had additional phosphorylation targets. MSK1 efficiently phosphorylates the HMGN1-S6A mutant, but not at all the triple-point mutant HMGN1-S6,20,24A (Figure 3D), an indication that this kinase targets S20,24. Phosphorylation at these sites has already been detected (Louie et al., 2000; Prymakowska-Bosak et al., 2001), and Western analysis verified that MSK1 targets these two serines (Figure 3E).

Phosphorylation of S20 and S24, located in the nucleosomal binding domain of HMGN1, abolishes the ability of the protein to bind to nucleosomes (Prymakowska-Bosak et al., 2001). By fluorescence recovery after photobleaching (FRAP) we demonstrated that in living cells the intranuclear mobility of the double-point mutant HMGN1-S20,24E, which mimics the phosphorylated state of the protein (Prymakowska-Bosak et al., 2001), is much faster than that of the wild-type protein. The intranuclear mobility is inversely proportional to the time that a protein resides on chromatin, reflecting the strength of its interaction with its chromatin binding site. Since MSK1 mediates the nucleosomal response and also phosphorylates the serines in the HMGN1 nucleosomal binding domain, we checked whether in living cells the nucleosomal response is associated with changes in the intranuclear mobility of HMGN1. We used FRAP to continuously monitor the mobility of HMGN1-GFP-fusion proteins before and during induction of the stress response. We expressed the relative mobility of the protein as the time needed to recover 80% (t80) of the HMGN1-GFP pre-bleach fluorescence intensity and as the relative intensity recovered 5 s after photobleaching

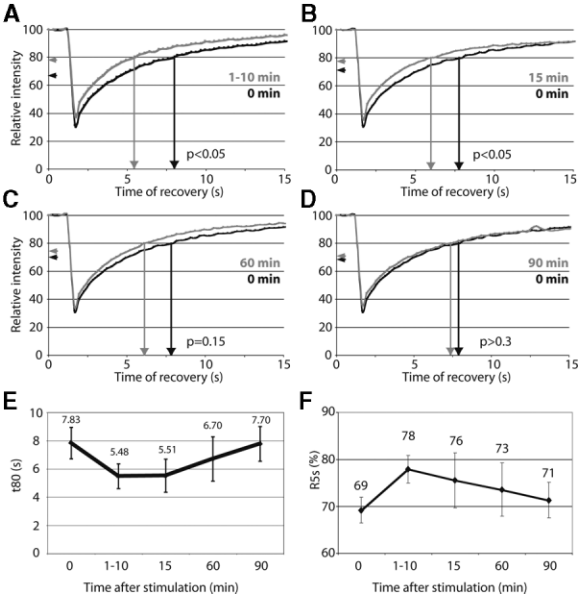

Figure 4. Decreased Chromatin Binding of HMGN1 after Anisomycin Stimulation

(A)–(D) Shown are quantitative FRAP analyses of HMGN1-GFP at the indicated times after stimulation with anisomycin (gray curves). Each panel contains the curve depicting the mobility of the protein before induction (black). The time needed to reach 80% of recovery (t80) is indicated by the arrows reaching the x axis. The recovery 5 s after stimulation (R5s) is indicated by the arrowheads pointing to the y axis. Curves are averages of 6–15 cells.

(E) and (F) Summary of the t80s and R5s from several experiments. Smaller values for t80s and larger values for R5s are indicative of faster mobility, i.e., decreased chromatin binding.

(R5s) (Catez et al., 2002). Prior to induction, the t80 and R5s of HMGN1-GFP were 7.83 s and 69%, respectively (Figure 4). Within the first 10 min of induction, the t80 dropped by 30% to 5.48 s, and the recovery reached almost 80%, indicating that the protein moved significantly faster. Fifteen minutes after induction, the t80 was 5.51 s and the R5s value remained close to 80%, indicating that the protein still moved faster than before the onset of the nucleosomal response. However, 60 min after induction, the mobility of the protein decreased; the t80 values were 6.7 s, and the R5s dropped to 73%. Finally, 90 min after induction, the mobility of the HMGN1-GFP was indistinguishable from that of the protein prior to induction, an indication that its chromatin interactions had recovered and were similar to those prior to anisomycin induction. Thus, stress induction is associated with a rapid increase in the HMGN1 mobility followed by a gradual decrease and recovery to original values. Since an increase in intranuclear mobility is indicative of a weaker chromatin binding, these results are consistent with a rapid and transient phosphorylation of the nucleosomal binding domain of HMGN1, leading to a temporary weakening in chromatin interactions (Figures 4E and 4F).

Phosphorylation of HMGN1 Precedes the Phosphorylation of H3

The anisomycin-induced increase in the intranuclear mobility of HMGN1 is relatively rapid and peaks before the phosphorylation of Ser6 in HMGN1 or S10 in H3 (compare Figure 1C to Figures 4E and 4F), raising the possibility that phosphorylation of S20,24 in HMGN1 is an early event in this phosphorylation cascade. Indeed, prior to stimulation strong immunofluorescence signals were obtained only with antibodies specific to mouse HMGN1, and very weak signals were observed with anti-P-S6-HMGN1 (Figure 5). After stimulation, we observed a gradual increase in the fluorescence intensity of the cells stained with antibodies specific to either P-S20,24-HMGN1, P-S6-HMGN1, or P-S10-H3. The fluorescence signals with these antibodies peaked, respectively, 15, 30, and 60 min after anisomycin treatment (Figures 5A–5E). Significantly, the anti-phospho-S20,24-HMGN1 peaked at the same time as the maximum rate of intranuclear mobility (compare Figures 4E and 4F to Figure 5A), supporting the conclusion that phosphorylation of the HMGN1 nucleosomal domain decreases its chromatin binding. Western analysis verified the presence of P-S20,24-HMGN1 in the extracts (see Supplemental Figure S1 at http://www.molecule.org/cgi/content/full/15/4/573/DC1/). Likewise, the immunofluorescence studies were in agreement with the Western analysis (Figure 1D), indicating that phosphorylation of S6-HMGN1 precedes that of S10-H3 (compare Figure 1D to Figure 5A). Thus, during the nucleosomal response, HMGN1 is rapidly and transiently phosphorylated, first in the nucleosomal binding domain at S20,24, followed by a less transient phosphorylation at S6. Phosphorylation of HMGN1 reduces its binding to chromatin thereby increasing the rate of H3 phosphorylation.

Immediate-Early Gene Expression in *Hmgn1*$^{-/-}$ Cells

As expected (Hazzalin et al., 1998), quantitative analysis by RNase protection of RNA extracted from *Hmgn1*$^{-/-}$ and *Hmgn1*$^{+/+}$ cells revealed that anisomycin treatment induced a transient elevation in the expression of all the 10 IE genes included in the *fos-jun* multi-probe template tested (not shown). The most significant difference between *Hmgn1*$^{-/-}$ and *Hmgn1*$^{+/+}$ cells was in the expression of *fosB* gene; the transcriptional response of this gene in cells devoid of HMGN1 protein was about twice that of *Hmgn1*$^{+/+}$ cells (Figure 6A). The expression of other genes was altered to a smaller degree or not at all, as exemplified by *c-jun* (Figure 6A). We broadened our examination for potential effects of HMGN1 on IE gene expression and used real-time RT-PCR to quantify the anisomycin-induced time course of expression of 18 genes selected from a list of IE-response genes (Murray et al., 2004). Hierarchal clustering (Eisen et al., 1998) of the ratios between mRNA expressed in *Hmgn1*$^{+/+}$ and *Hmgn1*$^{-/-}$ cells identified *RhoB* and *NGFr* as additional genes whose expression was induced to a higher level in *Hmgn1*$^{-/-}$ cells (Figure 6B). Thus, in 3 of the 18 genes examined (i.e., 15% of genes), the rate of anisomysin-induced transcription was higher in *Hmgn1*$^{-/-}$ than in *Hmgn1*$^{+/+}$ cells. Most of the genes were not affected, and in some genes, such as *Jun b* and *Fra 1*, the expression prior to anisomysin treatment was higher in *Hmgn1*$^{+/+}$ cells, but during induction the expression in *Hmgn1*$^{-/-}$ cells equaled that of *Hmgn1*$^{+/+}$ cells.

Chromatin immunoprecipitation (ChIP) experiments revealed that the increased anisomysin-induced tran-

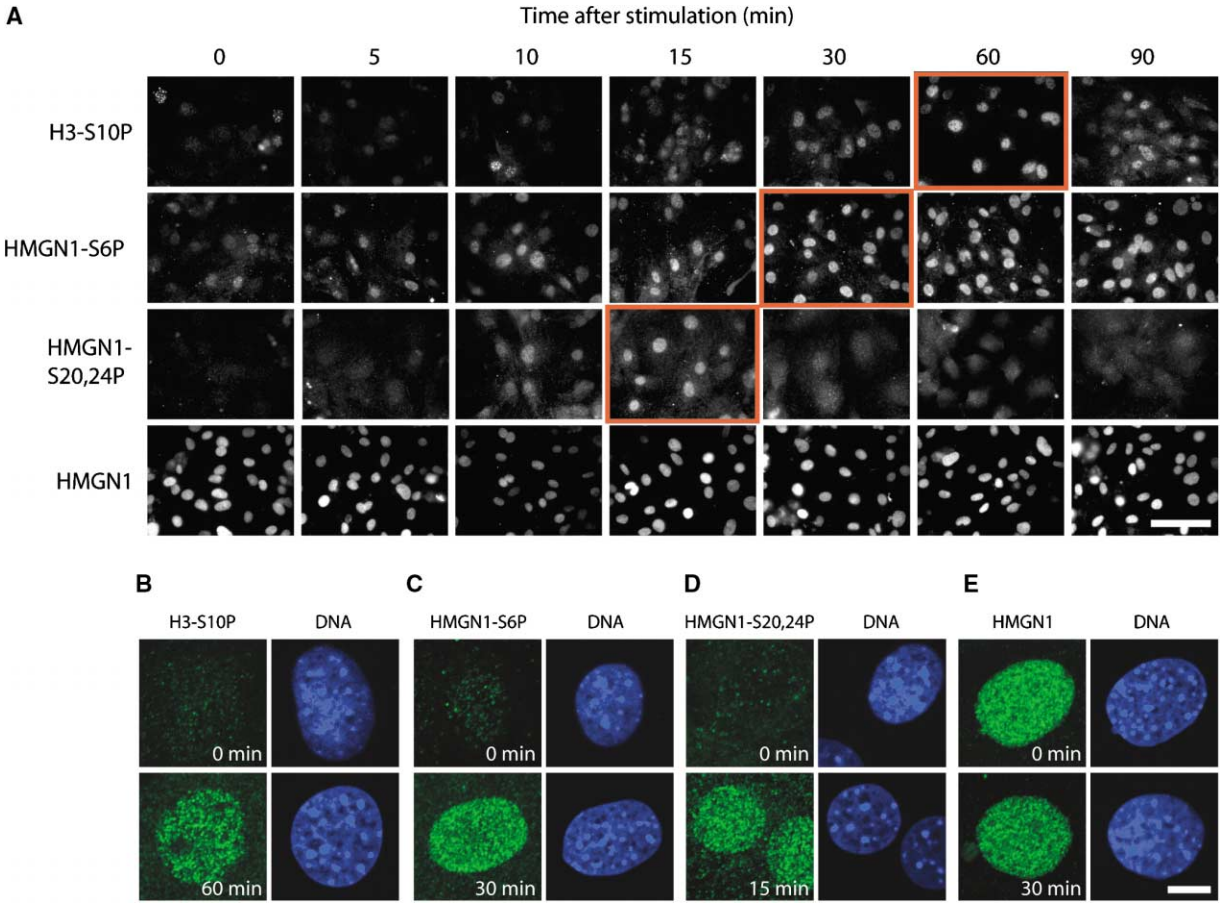

Figure 5. Sequential Phosphorylation of HMGN1 and H3 during the Nucleosomal Response to Anisomycin Treatment

(A) Immunofluorescence analysis with the antibodies specific to the epitopes, listed on the left, at various times after anisomycin stimulation. The panels boxed in red are the peaks of the immunofluorescence intensity for each set. Bar, 50 μm.

(B)–(E) Confocal images before stimulation (0 min) and at the peak of the signal with the antibody are listed on the top of the panel. Blue, DNA; Bar, 10 μm.

scriptional response of the *fosB* gene was associated with a rapid increase in the phosphorylation of S10-H3 on this gene (Figure 6C). The S10-H3 phosphorylation in this gene peaked in the *Hmgn1*$^{-/-}$ cells faster than in wild-type cells, a finding that is consistent with our observations that loss of HMGN1 enhances the overall rate of S10-H3 phosphorylation (compare to Figure 1C). In similar studies with *c-jun* representing an IE gene whose transcription was not different between *Hmgn1*$^{-/-}$ and *Hmgn1*$^{+/+}$ cells, we did not observe significant changes in the S10-H3 phosphorylation during IE induction.

The changes in the expression pattern and phosphorylation kinetics of the *fosB* and *c-jun* chromatin correlated with the presence of HMGN1 on these genes. Prior to IE gene induction, the occupancy of HMGN1 on the *fosB* gene was twice as high as its occupancy on actin or β-globin, two nontranscribed genes used for reference (Figure 6D). In contrast, *c-jun* and *c-fos* genes, whose expression in *Hmgn1*$^{-/-}$ was the same as in *Hmgn1*$^{+/+}$ cells, were not enriched in HMGN1 protein. Soon after anisomycin induction, the HMGN1 levels in the chromatin of the *fosB* gene, but not in the *c-fos* and *c-jun* genes, gradually decreased and within 30 min the abundance of the protein on *fosB* sequences was similar to that of the other genes examined. The decrease of HMGN1 occupancy on *fosB* was relatively fast, preceded the phosphorylation of S10-H3, and correlated with the phosphorylation and the increase in the intranuclear mobility of HMGN1. The higher occupancy of HMGN1 on the *fosB* gene may explain the difference in its expression in wild-type and *Hmgn1*$^{-/-}$ cells. Upon anisomycin treatment, the HMGN1 in the *fosB* gene is rapidly phosphorylated, its binding to chromatin reduced, the rate of S10-H3 phosphorylation increased, and the transcription levels elevated.

Discussion

We found that chromosomal protein HMGN1 modulates the levels of posttranslational modifications in the tails of histones and demonstrated that the interaction of HMGN1 with nucleosomes impedes the rate of phosphorylation of serine 10 in the amino terminus of histone H3. We suggest that structural nucleosome binding proteins such as HMGN1 affect the levels of posttranslational modification in the histone tails by modulating the

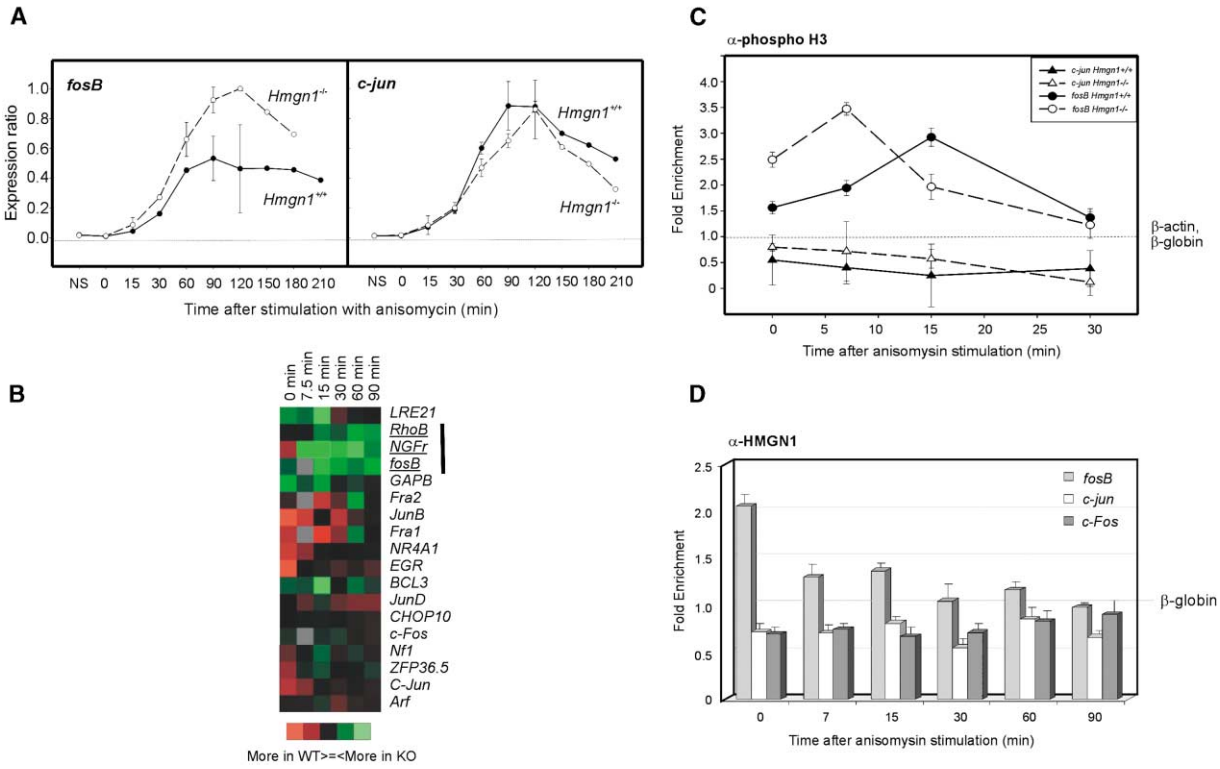

Figure 6. HMGN1 Modulates IE Gene Expression

(A) Loss of HMGN1 affects the expression level of *fosB* but not *c-jun*. Shown are the relative expressions of the two genes determined by quantitative RNase protection assays various times after anisomycin stimulation of MEF cell lines. The signals were normalized with GADPH and L32. The error bars represent the standard deviation at each time point calculated from triplicate experiments

(B) Cluster analysis (Eisen et al., 1998) of IE gene expression in $Hmgn1^{+/+}$ and $Hmgn1^{-/-}$ MEFs after anisomycin treatment. Higher expression in $Hmgn1^{+/+}$ cells is shown as red, in $Hmgn1^{-/-}$ as green, and equal expression as black. The pixels represent the log 2 ratios of the mRNA levels (determined by quantitative real-time RT-PCR). The underlined genes were hyperstimulated by anisomysin in $Hmgn1^{-/-}$ cells.

(C) HMGN1 modulates the phosphorylation of S10-H3 in *fosB* chromatin. Shown is the relative enrichment of *fosB* sequences in $Hmgn1^{+/+}$ chromatin immunoprecipitated with anti-S10-H3 various times after stimulation with anisomycin. The immunoprecipitates were analyzed by quantitative real-time PCR with specific primers for the genes indicated. The sequence abundances were normalized to β-globin and β-actin whose values were set to 1.

(D) Anisomycin-induced depletion of HMGN1 from *fosB* chromatin. Shown is the relative abundance of *fosB*, *c-jun*, and c-*fos* sequences in chromatin immunoprecipitated with anti-HMGN1 various times after stimulation with anisomycin.

ability of chromatin modifiers to access their nucleosomal targets.

Linking HMGN1 to Phosphorylation of Serine 10 in the H3 Tail

Several experiments linked the presence of HMGN1 protein to S10-H3 phosphorylation: first, the P-S10-H3 levels in growing $Hmgn1^{-/-}$ cells were higher than in wild-type $Hmgn1^{+/+}$ cells. Second, reexpression of wild-type, but not mutant, HMGN1 in the knockout cells lowered the amounts of P-S10-H3 to a level close to those found in normal cells. Third, loss of HMGN1 protein increased, and reexpression of HMGN1 reduced, the anisomycin-induced rate of S10-H3 phosphorylation in $Hmgn1^{-/-}$ cells. Fourth, phosphorylation of HMGN1 increased the intranuclear mobility of the protein and preceded the phosphorylation of S10-H3. Fifth, removal of HMGN1 from *fosB* chromatin preceded the phosphorylation of H3 in that gene.

The effect of HMGN1 is related to chromatin for several reasons: (1) wild-type HMGN1, but not the HMGN1-S20,24E mutant, restored the P-S10-H3 levels to normal; (2) HMGN1 inhibited the phosphorylation of nucleosomal, but not free, H3; (3) the maximum inhibition of phosphorylation by either MSK1 or RSK2 coincided with the maximum binding of HMGN1 to nucleosomes (Figure 2D); and (4) the HMGN1-S20,24E mutant, which does not bind to chromatin, did not inhibit phosphorylation, while deletion mutants that bind to chromatin do inhibit. HMGN1 is not a nonspecific inhibitor of either RSK2 or MSK1 since it did not affect the phosphorylation of free, nonnucleosomal H3. We also found that the overall phosphorylation of proteins in nuclear extracts of $Hmgn1^{+/+}$ cells was undistinguishable from that of $Hmgn1^{-/-}$ cells, an indication that loss of HMGN1 protein did not indiscriminately change the overall phosphorylation levels of nuclear proteins (not shown).

The "nucleosomal response," evoked by treating cells with various mitogens or stress-inducing agents, is one of the best-characterized links between signal transduction, S10-H3 phosphorylation, and gene activation. During the nucleosomal response, both H3 and HMGN1 are

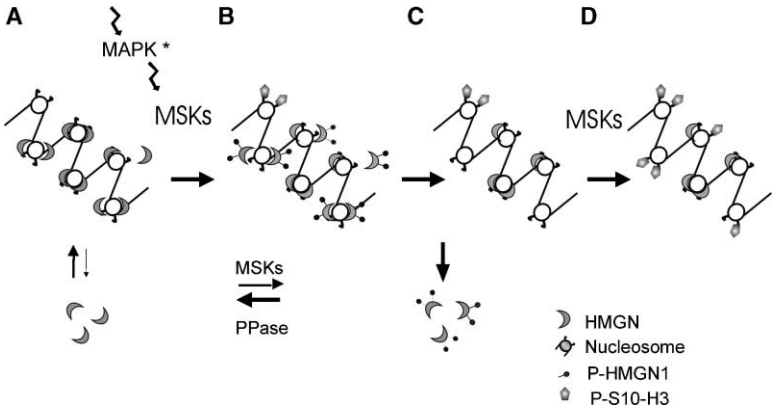

Figure 7. A Model Depicting HMGN1 Modulation of the Rate of Stress-Activated S10-H3 Phosphorylation

(A) In the nucleus HMGN1 binds transiently to nucleosomes.

(B) Anisomysin or similar stress signals activate MSKs who rapidly phosphorylate HMGN1.

(C) Phosphorylated HMGN1 does not bind to nucleosomes.

(D) Loss of HMGN1 enhances the rate of H3 phosphorylation. Note that phosphatases (PPase) remove the phosphate group from HMGN1.

transiently phosphorylated by MSK and perhaps RSK2 kinases. Our finding that the anisomycin, induced S10-H3 phosphorylation in *Hmgn1*$^{-/-}$ was faster than in *Hmgn1*$^{+/+}$ cells, and that re-expression of HMGN1 protein in *Hmgn1*$^{-/-}$ cells inhibited the rate of H3 phosphorylation (Figure 1E), provides evidence that HMGN1 indeed affects the posttranslational modification of histone H3. We have considered the possibility that the differences between the cell types reflect variations in cells' cycle arrest and progression. However, flow cytometry and BrdU incorporation analyses did not reveal any significant difference in the cell cycle progression between *Hmgn1*$^{-/-}$ and *Hmgn1*$^{+/+}$ cells (see Supplemental Figure S2 at http://www.molecule.org/cgi/content/full/15/4/573/DC1/).

We found that MSK1, one of the major mediators of the nucleosomal response, efficiently phosphorylates HMGN1 not only in S6 as previously reported but also at S20 and S24 located in the nucleosomal binding domain of the protein (Figure 3). Indeed, our immunofluorescence studies indicated that anisomycin treatment of cells induced a rapid and transient phosphorylation of S20 and S24 in HMGN1. Phosphorylation of S20,24 in HMGN1 has been detected in proteins extracted from growing cells (Louie et al., 2000) and is known to abolish the ability of the protein to bind to nucleosomes (Prymakowska-Bosak et al., 2001). Consistent with this observation, our FRAP analysis indicated that anisomycin induced a rapid and transient increase in the intranuclear mobility of HMGN1 (Figure 4), reflecting a weaker interaction between HMGN1 and nucleosomes. Significantly, the increased intranuclear mobility and the phosphorylation at HMGN1 S20,24 preceded the phosphorylation of S10-H3 (Figures 1D and 5). All of the data are consistent with the possibility that during the anisomycin-induced nucleosomal response HMGN1 is rapidly phosphorylated, a modification that decreases its binding to chromatin thereby exposing S10-H3 to increased phosphorylation.

FRAP analysis of living cells indicates that at any given time most of the HMGN1 is chromatin bound; however, the interactions of HMGN1 with chromatin are transient and the chromatin bound protein pool rapidly exchanges with the unbound pool, and HMGN1 protein moves rapidly from one binding site to another. It is likely that the phosphorylation of S20,24 occurs during the short periods in which HMGN1 is not directly bound to nucleosomes. This phosphorylation reduces the affinity constant of the entire cellular complement of HMGN1 to nucleosomes and facilitates the phosphorylation of S10-H3.

In summary, we suggest that the presence of HMGN1 on nucleosomes inhibits the ability of kinases to phosphorylate S10-H3. It is not presently clear whether the inhibition is due to steric hindrance at a specific site or to conformational changes that alter the interaction of the kinase complex with its target. During the nucleosomal response, MSK1 first phosphorylates residues in the nucleosomal binding domain of HMGN1, thereby reducing the binding of the protein to chromatin and enhancing the accessibility of S10-H3 to MSKs (Figure 7).

The Role of HMGN1 in IE Gene Expression

In response to external stimuli such as stress, cytokines, and growth factors, a set of genes collectively named immediate early (IE) genes, are rapidly and transiently activated (Bravo, 1990). Induction of IE gene expression correlates with MSK-mediated phosphorylation of serine residues in the amino terminus of H3 and S6 in HMGN1, an effect termed the "nucleosomal response" (Mahadevan et al., 1991; Thomson et al., 1999b). Although the nucleosomal response is well characterized, the role and significance of HMGN1 phosphorylation in IE gene expression has not been established. Our studies suggest that HMGN1 phosphorylation modulates the expression of a subset of the IE genes. This observation is in agreement with the recent finding that even in *MSK*$^{-/-}$ cells, where the phosphorylation of S10-H3 is dramatically reduced, the induction of IE genes is impaired but not abolished (Soloaga et al., 2003). Given that phosphorylation of S10-H3 is not an absolute requirement for an IE gene response, we would expect that loss of HMGN1 would alter rather than abolish IE gene expression.

We found that loss of HMGN1 affected the anisomysin response of 15% of the IE genes examined. The *fosB* gene expression in *Hmgn1*$^{-/-}$ cells was about 2-fold higher than in *Hmgn1*$^{+/+}$ cells. Prior to anisomycin stimulation, *fosB* chromatin was enriched in HMGN1 and upon stimulation the protein was rapidly released and S10-H3 was phosphorylated (Figure 6C and 6D). Lack of enrichment of HMGN1 in other IE genes such as *c-jun* does not necessarily mean that HMGN1 protein is not associated with these genes. The short residence time

of HMGN1 on any chromatin binding site may make it difficult to demonstrate enrichment of specific chromatin regions with this protein. Since the stress response involves the expression of many genes, it is likely that HMGN1 affects genes that have not yet been examined. Indeed, the stress response of *Hmgn1*$^{-/-}$ cells is significantly impaired and these cells are hypersensitive to various stress inducers such as UV exposure (Birger et al., 2003), heat shock, and X-ray (Y.B. and M.B., unpublished data).

HMGNs and the Histone Code

Although the existence of a histone code remains to be proven, it is well established that posttranslational modifications in the histone tails play an important role in chromatin-related processes. The levels of posttranslational modification at any residue in the histone tails reflect the equilibrium reached between enzymes that modify and demodify that residue. Inhibition of deacetylases or phosphatases elevates the levels of acetylation and phosphorylation in the histone tails, an indication of the continuous turnover of these modifications in nucleosomes. Our study suggests that the levels of modification could be affected not only by the activity of the modifying and demodifying enzymes but also by factors that affect the ability of the enzymes to access their nucleosomal targets. For HMGN, it is important to distinguish between the effect of the proteins on the compactness of the chromatin fiber and their effect on the local accessibility of a specific nucleosomal site. The binding of HMGN to nucleosomes reduces the compactness of the chromatin fiber and promotes overall accessibility to nucleosomes, but also alters the accessibility of unique sites in the nucleosomes to which they are bound. Thus, HMGN proteins enhance transcription, replication, and DNA repair in chromatin (Birger et al., 2003; Bustin, 2001), but reduce the rate of DNase1 digestion (Sandeen et al., 1980) and hydroxyl cleavage in nucleosomes (Alfonso et al., 1994).

Our study demonstrates that HMGN1 hinders the accessibility of specific kinases to S10-H3 in nucleosomes. Functional redundancy among members of the HMGN family may partially compensate for loss of HMGN1, raising the possibility that the role of HMGN1 is even larger than measured in the *Hmgn1*$^{-/-}$ cells. In addition to S10-H3, HMGN1 may also affect the phosphorylation of S28-H3 (Figure 2E), additional sites in H3 (Figure 1A), and H2A (Figure 2A), suggesting a wider role in the modulating histone posttranslational modifications.

We suggest that the binding of HMGN to nucleosomes leads to steric changes that could either enhance or inhibit the ability of chromatin-remodeling systems to reach their targets. Thus, HMGNs and perhaps similar nucleosome binding proteins modulate the levels of posttranslational modifications in the histone tails.

Experimental Procedures

Materials

Antibodies and kinases were from Upstate Biotechnology. Antibodies to histones and HMGN mutants were described (Prymakowska-Bosak et al., 2001). EGF and anisomycin were from Gibco.

Cell Culture and Western Blotting

Hmgn1$^{-/-}$ and *Hmgn1*$^{+/+}$ MEFs and stable revertant *Hmgn1*$^{-/-}$ expressing HMGN1 proteins under the control of the TRE element were grown as described (Birger et al., 2003). After reaching 90% confluence, the cells were made quiescent by growing in serum-deprived medium (DMEM, 0.1% serum) for 48 to 72 hr prior to the addition of 50 ng/ml anisomycin. Starvation did not totally abolish the phospho S10-H3 levels. For Westerns, cells were scraped with 1× SDS sample buffer (45 mM Tris-HCl, 1 mM EDTA, 1% SDS, 2 mM DTT, 10% glycerol, 0.01% bromophenol blue, protease inhibitor cocktail, 50 nM okadaic acid, 100 μM sodium orthovanadate, 10 mM sodium butyrate, and 0.5 μg/ml of TSA), the amount of protein in each extract equalized, and the proteins resolved by SDS-PAGE again transferred onto PVDF membranes (Lim et al., 2004).

RNase Protection Assay

Ten micrograms of total RNA prepared with TRIZOL (Invitrogen) was probed with the *fos-jun* multi-probe template sets (BD Pharmingen), which was transcribed using the T7/SP6 RiboQuant in vitro Transcription Kit (BD Pharmingen) in the presence of [α-^{32}P]UTP. The protected fragments were fractionated on 5% 7 M urea acrylamide gels. Transferred gels were scanned with a PhosphorImager and quantified with the ImageQuant program (Molecular Dynamics). The signals were normalized using the signals for GAPDH and L32 mRNAs.

In Vitro Phosphorylation Assay

CP (1 μg per reaction) were incubated for 30 min at 30°C with increasing amounts of HMGN1 in the phosphorylation buffer recommended by the manufacturer containing 0.1 μCi [γ-^{32}P]ATP, and the reaction analyzed as described (Prymakowska-Bosak et al., 2001).

ChIP and Real-Time Quantitative PCR

ChIP experiments were performed as previously described (Birger et al., 2003). Each experiment was done with at least two different clones, and each ChIP was analyzed at least three times.

Immunofluorescence and FRAP Analysis

Various antibodies were applied to different areas of the same slide, and imaging for all time points was performed under identical conditions and exposure settings either by confocal imaging as described previously (Catez et al., 2002; Prymakowska-Bosak et al., 2002) or by Epi-fluorescence with an Orca ER CCD camera (Hamamatsu). For FRAP experiments (Catez et al., 2002) single images were collected every 296 ms over 15 s. Routinely, 6–15 cells were used for FRAP before anisomycin stimulation, and 6–7 cells were used for FRAP for each time point. For the first 10 min after stimulation, FRAP curves were generated at 1 min intervals. The student's t test was used to determine the significance of the results.

IE Genes Expression Profiling and Hierarchical Clustering Analysis

Real-time quantitative RT-PCR was done with an ABI PRISM 7900HT using β-actin, ACP, and β-globin for normalization. Cluster and Treeview (Eisen et al., 1998) software were used for computation and graphical representation of the gene clusters.

Supplemental Data

Supplemental Data, including additional data and detailed Experimental Procedures used in this work, are available at http://www.molecule.org/cgi/content/full/15/4/573/DC1/.

Acknowledgments

We thank Ms Susan H. Garfield and Mr. Stephen M. Wincovitch for help with confocal microscopy.

Received: November 26, 2003
Revised: June 1, 2004
Accepted: June 10, 2004
Published: August 26, 2004

References

Alfonso, P.J., Crippa, M.P., Hayes, J.J., and Bustin, M. (1994). The footprint of chromosomal proteins HMG-14 and HMG-17 on chromatin subunits. J. Mol. Biol. *236*, 189–198.

Barratt, M.J., Hazzalin, C.A., Zhelev, N., and Mahadevan, L.C. (1994). A mitogen- and anisomycin-stimulated kinase phosphorylates HMG-14 in its basic amino-terminal domain in vivo and on isolated mononucleosomes. EMBO J. *13*, 4524–4535.

Birger, Y., West, K.L., Postnikov, Y.V., Lim, J.H., Furusawa, T., Wagner, J.P., Laufer, C.S., Kraemer, K.H., and Bustin, M. (2003). Chromosomal protein HMGN1 enhances the rate of DNA repair in chromatin. EMBO J. *22*, 1665–1675.

Bravo, R. (1990). Growth factor-responsive genes in fibroblasts. Cell Growth Differ. *1*, 305–309.

Bustin, M. (2001). Chromatin unfolding and activation by HMGN(*) chromosomal proteins. Trends Biochem. Sci. *26*, 431–437.

Catez, F., Brown, D.T., Misteli, T., and Bustin, M. (2002). Competition between histone H1 and HMGN proteins for chromatin binding sites. EMBO Rep. *3*, 760–766.

Chadee, D.N., Hendzel, M.J., Tylipski, C.P., Allis, C.D., Bazett-Jones, D.P., Wright, J.A., and Davie, J.R. (1999). Increased Ser-10 phosphorylation of histone H3 in mitogen-stimulated and oncogene-transformed mouse fibroblasts. J. Biol. Chem. *274*, 24914–24920.

Cheung, P., Allis, C.D., and Sassone-Corsi, P. (2000). Signaling to chromatin through histone modifications. Cell *103*, 263–271.

Clayton, A.L., and Mahadevan, L.C. (2003). MAP kinase-mediated phosphoacetylation of histone H3 and inducible gene regulation. FEBS Lett. *546*, 51–58.

Clayton, A.L., Rose, S., Barratt, M.J., and Mahadevan, L.C. (2000). Phosphoacetylation of histone H3 on c-fos- and c-jun-associated nucleosomes upon gene activation. EMBO J. *19*, 3714–3726.

Crippa, M.P., Alfonso, P.J., and Bustin, M. (1992). Nucleosome core binding region of chromosomal protein HMG-17 acts as an independent functional domain. J. Mol. Biol. *228*, 442–449.

Davie, J.R. (2003). MSK1 and MSK2 mediate mitogen- and stress-induced phosphorylation of histone H3: a controversy resolved. Sci. STKE *2003*, PE33. 10.1126/stke.2003.195.pe33.

Davie, J.R., and Spencer, V.A. (2001). Signal transduction pathways and the modification of chromatin structure. Prog. Nucleic Acid Res. Mol. Biol. *65*, 299–340.

Eisen, M.B., Spellman, P.T., Brown, P.O., and Botstein, D. (1998). Cluster analysis and display of genome-wide expression patterns. Proc. Natl. Acad. Sci. USA *95*, 14863–14868.

Hazzalin, C.A., Le Panse, R., Cano, E., and Mahadevan, L.C. (1998). Anisomycin selectively desensitizes signalling components involved in stress kinase activation and fos and jun induction. Mol. Cell. Biol. *18*, 1844–1854.

Herrera, J., Sakaguchi, K., Bergel, M., Trieschmann, L., Nakatani, Y., and Bustin, M. (1999). Specific acetylation of chromosomal protein HMG-17 by P/CAF alters its interaction with nucleosomes. Mol. Cell. Biol. *19*, 3466–3473.

Herrera, J.E., West, K.L., Schiltz, R.L., Nakatani, Y., and Bustin, M. (2000). Histone H1 is a specific repressor of core histone acetylation in chromatin. Mol. Cell. Biol. *20*, 523–529.

Horn, P.J., Carruthers, L.M., Logie, C., Hill, D.A., Solomon, M.J., Wade, P.A., Imbalzano, A.N., Hansen, J.C., and Peterson, C.L. (2002). Phosphorylation of linker histones regulates ATP-dependent chromatin remodeling enzymes. Nat. Struct. Biol. *9*, 263–267.

Jenuwein, T., and Allis, C.D. (2001). Translating the histone code. Science *293*, 1074–1080.

Labrador, M., and Corces, V.G. (2003). Phosphorylation of histone H3 during transcriptional activation depends on promoter structure. Genes Dev. *17*, 43–48.

Lim, J.H., Catez, F., Birger, Y., Postnikov, Y., and Bustin, M. (2004). Preparation and functional analysis of HMGN proteins. Methods Enzymol. *375*, 323–342.

Louie, D.F., Gloor, K.K., Galasinski, S.C., Resing, K.A., and Ahn, N.G. (2000). Phosphorylation and subcellular redistribution of high mobility group proteins 14 and 17, analyzed by mass spectrometry. Protein Sci. *9*, 170–179.

Mahadevan, L.C., Willis, A.C., and Barratt, M.J. (1991). Rapid histone H3 phosphorylation in response to growth factors, phorbol esters, okadaic acid, and protein synthesis inhibitors. Cell *65*, 775–783.

Murray, J.I., Whitfield, M.L., Trinklein, N.D., Myers, R.M., Brown, P.O., and Botstein, D. (2004). Diverse and specific gene expression responses to stresses in cultured human cells. Mol. Biol. Cell *15*, 2361–2374.

Prymakowska-Bosak, M., Misteli, T., Herrera, J.E., Shirakawa, H., Birger, Y., Garfield, S., and Bustin, M. (2001). Mitotic phosphorylation prevents the binding of HMGN proteins to chromatin. Mol. Cell. Biol. *21*, 5169–5178.

Prymakowska-Bosak, M., Hock, R., Catez, F., Lim, J.H., Birger, Y., Shirakawa, H., Lee, K., and Bustin, M. (2002). Mitotic phosphorylation of chromosomal protein HMGN1 inhibits nuclear import and promotes interaction with 14.3.3 proteins. Mol. Cell. Biol. *22*, 6809–6819.

Sandeen, G., Wood, W.I., and Felsenfeld, G. (1980). The interaction of high mobility proteins HMG14 and 17 with nucleosomes. Nucleic Acids Res. *8*, 3757–3778.

Sassone-Corsi, P., Mizzen, C.A., Cheung, P., Crosio, C., Monaco, L., Jacquot, S., Hanauer, A., and Allis, C.D. (1999). Requirement of Rsk-2 for epidermal growth factor-activated phosphorylation of histone H3. Science *285*, 886–891.

Shibata, K., and Ajiro, K. (1993). Cell cycle-dependent suppressive effect of histone H1 on mitosis-specific H3 phosphorylation. J. Biol. Chem. *268*, 18431–18434.

Soloaga, A., Thomson, S., Wiggin, G.R., Rampersaud, N., Dyson, M.H., Hazzalin, C.A., Mahadevan, L.C., and Arthur, J.S. (2003). MSK2 and MSK1 mediate the mitogen- and stress-induced phosphorylation of histone H3 and HMG-14. EMBO J. *22*, 2788–2797.

Strahl, B.D., and Allis, C.D. (2000). The language of covalent histone modifications. Nature *403*, 41–45.

Thomson, S., Clayton, A.L., Hazzalin, C.A., Rose, S., Barratt, M.J., and Mahadevan, L.C. (1999a). The nucleosomal response associated with immediate-early gene induction is mediated via alternative MAP kinase cascades: MSK1 as a potential histone H3/HMG-14 kinase. EMBO J. *18*, 4779–4793.

Thomson, S., Mahadevan, L.C., and Clayton, A.L. (1999b). MAP kinase-mediated signalling to nucleosomes and immediate-early gene induction. Semin. Cell Dev. Biol. *10*, 205–214.

Trieschmann, L., Postnikov, Y., Rickers, A., and Bustin, M. (1995). Modular structure of chromosomal proteins HMG-14 and HMG-17: definition of a transcriptional activation domain distinct from the nucleosomal binding domain. Mol. Cell. Biol. *15*, 6663–6669.

Trieschmann, L., Martin, B., and Bustin, M. (1998). The chromatin unfolding domain of chromosomal protein HMG-14 targets the N-terminal tail of histone H3 in nucleosomes. Proc. Natl. Acad. Sci. USA *95*, 5468–5473.

Turner, B.M. (2002). Cellular memory and the histone code. Cell *111*, 285–291.

Yamamoto, Y., Verma, U.N., Prajapati, S., Kwak, Y.T., and Gaynor, R.B. (2003). Histone H3 phosphorylation by IKK-alpha is critical for cytokine-induced gene expression. Nature *423*, 655–659.